AFRL-RY-WP-TP-2014-0294

LIMIT-CYCLE DYNAMICS WITH REDUCED SENSITIVITY TO PERTURBATIONS -POSTPRINT

Nicholas G. Usechak and Vassilios Kovanis
Optoelectronics Technology Branch
Aerospace Components & Subsystems Division

Thomas B. Simpson
L-3 Applied Technologies, Inc.

Jia-Ming Liu and Mohammad AlMulla
University of California Los Angeles

JANUARY 2015
Interim

Approved for public release; distribution unlimited.

See additional restrictions described on inside pages

STINFO COPY

AIR FORCE RESEARCH LABORATORY
SENSORS DIRECTORATE
WRIGHT-PATTERSON AIR FORCE BASE, OH 45433-7320
AIR FORCE MATERIEL COMMAND
UNITED STATES AIR FORCE

REPORT DOCUMENTATION PAGE

Form Approved
OMB No. 0704-0188

1. REPORT DATE *(DD-MM-YY)*
January 2015

2. REPORT TYPE
Journal Article Postprint

3. DATES COVERED *(From - To)*
1 December 2012 – 1 December 2013

4. TITLE AND SUBTITLE
LIMIT-CYCLE DYNAMICS WITH REDUCED SENSITIVITY TO PERTURBATIONS - POSTPRINT

5a. CONTRACT NUMBER
In-House

5b. GRANT NUMBER

5c. PROGRAM ELEMENT NUMBER
61102F

6. AUTHOR(S)
Nicholas G. Usechak and Vassilios Kovanis (AFRL/RYDH)
Thomas B. Simpson (L-3 Applied Technologies, Inc.)
Jia-Ming Liu and Mohammad AlMulla (University of California Los Angeles)

5d. PROJECT NUMBER
2305

5e. TASK NUMBER
DP

5f. WORK UNIT NUMBER
Y05T

7. PERFORMING ORGANIZATION NAME(S) AND ADDRESS(ES)

Optoelectronics Technology Branch
Aerospace Components & Subsystems Division
Air Force Research Laboratory, Sensors Directorate
Wright-Patterson Air Force Base, OH 45433-7320
Air Force Materiel Command, United States Air Force

L-3 Applied Technologies, Inc.

University of California Los Angeles

8. PERFORMING ORGANIZATION REPORT NUMBER
AFRL-RY-WP-TP-2014-0294

9. SPONSORING/MONITORING AGENCY NAME(S) AND ADDRESS(ES)

Air Force Research Laboratory
Sensors Directorate
Wright-Patterson Air Force Base, OH 45433-7320
Air Force Materiel Command
United States Air Force

10. SPONSORING/MONITORING AGENCY ACRONYM(S)
AFRL/RYDH

11. SPONSORING/MONITORING AGENCY REPORT NUMBER(S)
AFRL-RY-WP-TP-2014-0294

12. DISTRIBUTION/AVAILABILITY STATEMENT
Approved for public release; distribution unlimited.

13. SUPPLEMENTARY NOTES
Journal article published in American Physical Society, Physical Review Letters 112, 023901. © 2014 American Physical Society. The U.S. Government is joint author of the work and has the right to use, modify, reproduce, release, perform, display or disclose the work. PAO case number 88ABW-2013-2676, Clearance Date 6 June 2013. Report contains color.

14. ABSTRACT
Limit-cycle oscillators are used to model a broad range of periodic nonlinear phenomena. Using the optically injected semiconductor laser as a paradigmatic example, we demonstrate that at specific operating points, the period-one oscillation frequency is simultaneously insensitive to multiple perturbation sources. In our system these include the temperature fluctuations experienced by the master and slave lasers as well as fluctuations in the bias current applied to the slave laser. Tuning of the oscillation frequency then depends only on the injected optical field amplitude. Experimental measurements are in detailed quantitative agreement with numerical modeling. These special operating points should prove valuable for developing ultrastable nonlinear oscillators, such as a narrow-linewidth, frequency-tunable photonic microwave oscillator.

15. SUBJECT TERMS
oscillators, semiconductor laser

16. SECURITY CLASSIFICATION OF: a. REPORT	b. ABSTRACT	c. THIS PAGE	17. LIMITATION OF ABSTRACT:	18. NUMBER OF PAGES	19a. NAME OF RESPONSIBLE PERSON (Monitor)
Unclassified	Unclassified	Unclassified	SAR	8	Nicholas Usechak

19b. TELEPHONE NUMBER *(Include Area Code)*
937-528-8851

Limit-Cycle Dynamics with Reduced Sensitivity to Perturbations

Thomas B. Simpson,[1,*] Jia-Ming Liu,[2] Mohammad AlMulla,[2] Nicholas G. Usechak,[3] and Vassilios Kovanis[3]

[1] *L-3 Applied Technologies, Inc., 10770 Wateridge Circle, San Diego, CA*

[2] *Electrical Engineering Department, University of California, Los Angeles, Los Angeles, CA*

[3] *Air Force Research Laboratory, 2241 Avionics Circle, Wright–Patterson AFB, OH*

(Dated: May 23, 2013)

Limit-cycle oscillators are used to model a broad range of periodic nonlinear phenomena. Using the optically-injected semiconductor laser as a paradigmatic example, we demonstrate that at specific operating points, the period-one oscillation frequency is simultaneously insensitive to multiple perturbation sources. In our system these include the temperature fluctuations experienced by the master and slave lasers as well as fluctuations in the bias current applied to the slave laser. Tuning of the oscillation frequency then depends only on the injected optical field amplitude. Experimental measurements are in detailed quantitative agreement with numerical modeling. These special operating points should prove valuable for developing ultrastable nonlinear oscillators, such as a narrow-linewidth, frequency-tunable photonic microwave oscillator.

Nonlinear dynamics in oscillators has been invoked to explain a wide variety of physical phenomena over disciplines ranging from neuroscience to geoscience [1]. Systems and devices exhibiting self-sustained oscillations, described mathematically as a limit cycle, are fundamental components in complex systems such as biological oscillators and technological applications such as time/frequency references, and there currently is considerable interest in photonic implementations [2]. In all of these instances, there is the need to understand the influence of a noisy/perturbing environment on the properties of the limit cycle. Perturbations in oscillatory systems can be translated in frequency through the nonlinear coupling among elements. For example, low-frequency vibration or temperature perturbations can negatively impact the stability of a high-frequency oscillator.

Here we demonstrate that nonlinear dynamics, which usually degrades system performance, can counterintuitively be used to suppress the deleterious effects such perturbations have on performance through a proper choice of the operating point of the system. Using an optically-injected semiconductor laser, we confirm that at certain operating points the fundamental resonance frequency of the system, the so-called period-one (P1) frequency, possess greatly reduced sensitivity to current fluctuations in the slave laser and/or to perturbations in the operating temperatures of either laser. These variations would normally lead to optical frequency fluctuations of the free-running lasers. Effectively, at these points the tuning of the P1 frequency is controlled by the amplitude of the injected optical signal alone. This is in stark contrast to the beat signal generated at a photodiode simultaneously subject to two free-running lasers, where the frequency of the current oscillations due to interference is controlled simply by their frequency detuning. This system provides a concrete physical platform to investigate the role of nonlinear dynamics in controlling sensitivity to external perturbations, and should therefore provide an additional avenue to be exploited in the creation of low phase-noise sources e.g. tunable photonic oscillators.

Model systems for nonlinear dynamics, where detailed quantitative comparisons between model and the real physical system can be made, are particularly useful to understand the complexities introduced by nonlinearities in the actual system. Optically-injected semiconductor lasers have been shown to exhibit a wide range of generic dynamic characteristics due to the nonlinearities inherent in the coupled optical-field/free-carrier system [3]. These characteristics have been quantitatively recovered using a three-dimensional, lumped-element, detuned-oscillator model of the coupling between the circulating optical field and the carrier density in the gain medium [3–5]:

$$\dot{x} = zx + (bz - \omega)y + \xi \quad (1)$$

$$\dot{y} = zy - (bz - \omega)x \quad (2)$$

$$\dot{z} = \kappa - Az - B(1 + 2z)(x^2 + y^2 - 1) \quad (3)$$

These equations describe a system of three coupled elements, two (x, y) with conjugate coupling, and a third, z, exciting the other two while being damped by them, along with various external control and coupling/biasing parameters. For the specific case of the optically-injected semiconductor laser, x and y are proportional to the quadrature components of the circulating optical field, and z is proportional to the carrier density of the gain medium. The parameters ξ and ω describe the normalized amplitude and detuning (relative to the free-running slave laser) of the injected optical field, respectively, while κ is an externally applied injection current beyond the steady-state bias. The parameter b is intrinsic to the injected laser and is the ratio of the real and imaginary parts of the complex refractive index variation with carrier density, while A and B describe coupling terms that depend on the steady-state bias current. All parameters except b can be widely varied for a single laser experimentally simply by changing its applied current and operating temperature. Nevertheless, due to fabrication issues, b is found to vary between lasers. Therefore, this system is capable of simulating a wide range of external coupling and internal cross-coupling. The key control parameters

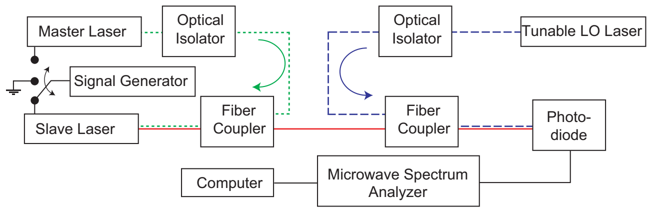

FIG. 1: Schematic of a semiconductor laser subject to external optical injection (doted green). The master laser is isolated from feedback. In our experiment, the output from the injected laser (solid red) is detected by a fast photodiode and monitored using a microwave spectrum analyzer. A small-signal modulation current is added to either the master or slave laser. A tunable laser acting as a local oscillator (LO) can be added to generate a high-resolution optical spectrum using a heterodyne technique (dashed blue).

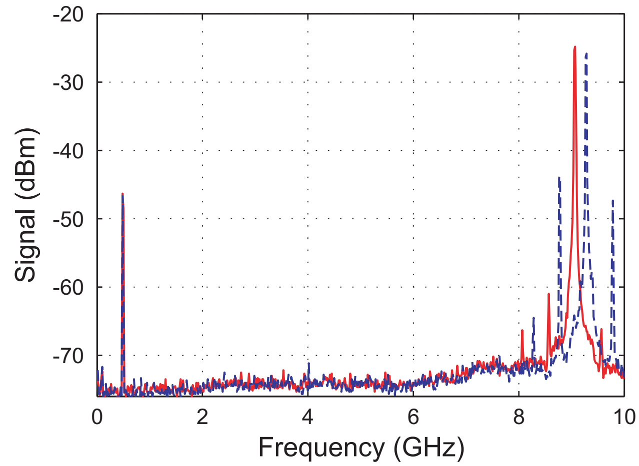

FIG. 2: Power spectra of the laser output in the P1 oscillation regime with the addition of a weak modulation current to the slave laser. The sidebands are minimized when the master laser is detuned to generate a local minimum of the P1 frequency (solid red, detuning = -2.1 GHz), but are much stronger for a shifted detuning frequency (dashed blue, detuning = -1.2 GHz). A normalized injection amplitude of 0.06 is used in both cases and the peak at the modulation frequency (500 MHz) remains essentially unchanged.

for these dynamics are the amplitude and detuning between the injected signal from the master laser relative to the free-running slave laser characteristics. Over a wide range of these two control parameters, the output of the injected slave laser is a periodic oscillation at the P1 frequency of the system [3, 4].

Figure 1 is a schematic of the configuration of an externally-injected semiconductor laser. The output of a steady-state single-mode master laser, at an optical frequency ν_i, passes through an isolator and is injected into the oscillating mode of a second semiconductor laser (the so-called slave laser), also steady-state and single mode, with a free-running frequency ν_0. A weak modulation current can be added to either the master or slave laser for diagnostic purposes. The slave laser under investigation is a fiber-pigtailed DFB laser operating at a wavelength of 1557 nm that has been extensively investigated previously [3]. The different components are all fiber coupled with SMF-28 optical fiber. An amplified fast photodiode detects the output and the power spectrum of the photodiode signal is monitored using a microwave spectrum analyzer (MSA). A third laser is sometimes used as a tunable local oscillator to generate a heterodyne signal that effectively converts the MSA into an optical spectrum analyzer [3].

When displaying a P1 dynamic, the optical spectrum consists of dominant peaks at the injection frequency and at one resonance frequency (f_0) below, which is the injection-perturbed oscillation frequency of the slave laser. In addition, other weaker peaks at periodic offsets of the P1 frequency are typically present. The addition of a weak modulation current at a frequency $f_m \ll f_0$ causes sidebands to appear about these main optical peaks. Figure 2 shows typical power spectra. The power spectrum displays a single dominant peak at the P1 oscillation/pulsation frequency, along with sidebands and a peak at the modulation frequency if a modulation current is present. With no modulation current, only the dominant peak at the P1 frequency appears in the power spectrum, and the optical spectrum displays only the discrete set of peaks offset by this frequency.

For these experiments, the operating points of the master and slave lasers are temperature tuned so the P1 frequency is locally insensitive to the master-slave detuning; the P1 frequency is at a local minimum with respect to this control parameter and, therefore, insensitive to temperature fluctuations. A weak sinusoidal modulation current with frequency $f_m \ll f_0$ is then added to either the master or slave laser. Typically, the P1 frequency peak develops sidebands offset by integer multiples of f_m regardless of which laser the modulation current is added to. However, at approximately the detuning that produces the minimum P1 frequency we observe a minimum in the amplitude of the modulation sidebands in the power spectrum when the modulation current is added to the slave laser, as shown in Fig. 2. By comparison, the peak at the modulation frequency shows no such minimum, verifying that the linear response of the laser is unchanged. If the modulation current is added to the master laser, there is a less pronounced modulation minimum, but it occurs at a detuning well offset from the operating point where the P1 frequency is minimized.

Figure 3 shows experimental measurements of the amplitude of the sidebands and the P1 frequency as the detuning frequency of the master laser is stepped through the P1 frequency minimum. Here the amplitude of the P1 frequency peak varies strongly as the detuning moves away from the Hopf bifurcation. Therefore, the amplitudes of the sidebands are shown normalized to the amplitude of the central peak at each detuning. The error for the experimentally measured detuning is ±300 MHz

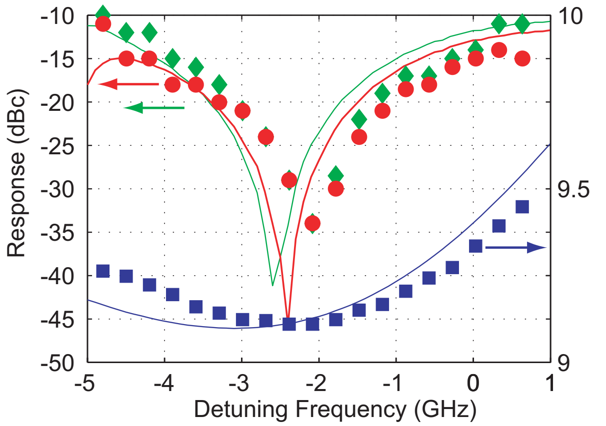

FIG. 3: Experimentally measured (symbols) and calculated (solid curves) values of the modulation sideband amplitude and the P1 frequency using a normalized injection amplitude of 0.06. This figure shows the positive frequency detuning sideband (red circles), the negative detuning sideband (green diamonds), and the corresponding P1 frequency (blue squares).

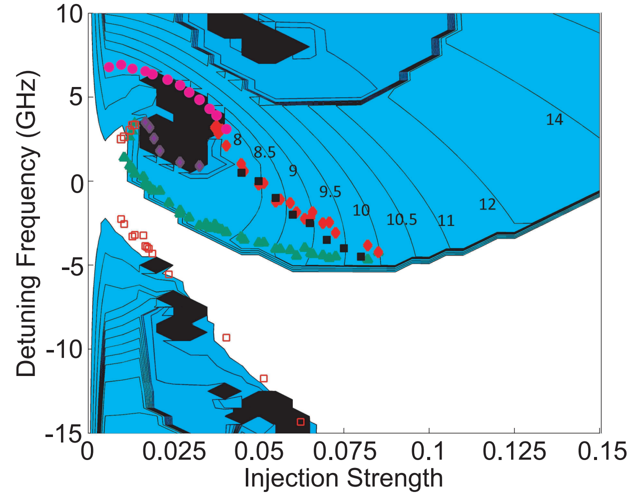

FIG. 4: Mapping of key transitions of the injected laser as a function of the detuning frequency and amplitude of the master. Experimental Data – the open squares are the Saddle-Node bifurcation points that, along with the green triangles representing Hopf Bifurcation points, bound the region of stable locking, the red diamonds mark operating points with a local P1 minimum frequency. The pink circles denote a saddle-node bifurcation of limit cycles, either from P1 to more complex dynamics or between two P1 frequencies, and the purple diamonds, alternate routes from P1 to more complex dynamics. Calculated Data – the light blue regions mark P1, and the dark blue regions P2, periodic dynamics with lines of constant frequency are labeled in GHz. The white region denotes stable operation, while the black represents complex dynamics. The black squares denote the calculated positions of the local P1 minima to be compared with the red diamonds.

while the depths of the minima were limited by the background noise levels. The dips in the amplitudes of the sidebands are quite narrow with respect to the relaxation rates of the free-running laser which are $> 10^9 s^{-1}$ at this operating point [3, 5]. Further, additional measurements made on signals of broader bandwidth (> 10 MHz) up to modulation frequencies of 100 MHz showed an equivalent dip in the amplitude. Therefore, there is reduced sensitivity to all low-frequency fluctuations in the injection current of the slave laser simultaneously with the reduced sensitivity to fluctuations in the master-slave detuning.

Figure 4 shows a mapping of key operating points of the laser, comparing experimental measurements with model calculations (described later), as functions of the master laser detuning from the free-running slave optical frequency and the amplitude of the injected signal. The mapping is made by monitoring the power and optical spectra of the optically-injected laser. Saddle-node and Hopf bifurcations bound the region of stable locking, with the Hopf bifurcation leading to P1 limit-cycle oscillation. More complex dynamics occur in the region between the points labeled as either the saddle-node bifurcation of limit cycles or alternate routes to chaos (through period doubling or other routes). One cannot identify the saddle node bifurcation of limit cycles through the spectra, but previous work using bifurcation analysis has done so [4]. Along the other boundary, period-doubling routes to chaos have been identified [3].

To produce the quantitative comparisons between data and theory we modeled the optically-injected laser using a set of coupled equations, of the form of Eqs. 1–3, for the circulating field amplitude of the oscillating laser mode and the carrier density of the gain medium [3, 6]. This model modifies Eqs. 1–3 by adding the effects of gain saturation to both the real (refractive index) and imaginary (gain) parts of the nonlinear susceptibility [3]. The numerical simulations used a Runge–Kutta integration procedure over durations $> 1\mu s$ to generate time series that were subsequently Fourier transformed to produce spectra [6].

The results of the numerical calculations are shown in Figs. 3 and 4 using parameters that have been determined experimentally for the laser under investigation [5]. The model fully reproduces the bifurcation boundaries of the P1 region, the local minimum in the P1 frequency, and the simultaneous dip in the amplitude of the sidebands as the detuning between master and slave lasers is changed. The positions of the P1 frequency minimum and the amplitude dip are sensitive to the effects of gain saturation; to obtain good agreement between experimentally measured data and the model saturation effects were included. More details on the comparison of the model and experimental data, particularly optical spectra, will be given in a later publication. Here, we note that the basic observation of simultaneous insensitivity to perturbations in the detuning between master and slave and to perturbations in the slave laser current remained when

gain saturation effects were removed, confirming that this term in the model is not necessary to generate the underlying interaction, only to achieve quantitative agreement between our numerical model and experiment.

It is important to remember that the sidebands in the power spectrum are the sum of terms due to the mixing of the sidebands in the optical spectrum with adjacent central peaks. By comparing the power spectra with optical spectra generated simultaneously using the hetrodyne technique, we verified that the sharp minima in the sidebands (see Fig. 3) result primarily from the interference of the multiple wave-mixing contributions, not the simultaneous reduction in the amplitude of the sidebands of each optical peak. The component at the modulation frequency, which results from the sum of the mixing of each optical sideband with its respective central peak, remains essentially constant as the injection detuning frequency is changed.

While the effects of current noise on the P1 frequency are suppressed, spontaneous emission noise still plays a role. One can see this in the model by considering spontaneous emission as a fluctuating source term with contributions to both the optical field and carrier density equations [7]. The carrier-equation contribution is eliminated through the interference of wave-mixing terms described above, as if it were an injection current modulation source, while the field-equation contribution, which acts like a stochastic external optical injection term, still contributes. However, only the amplitude fluctuations, not the phase/frequency fluctuations, contribute, leading to the Lorentzian lineshape of the spectral features in Fig. 2. Previously, it was shown how the coupling of optical fields and free carriers in a semiconductor laser could lead to reduced power fluctuations [7]. In the optically-injected laser, the nonlinear dynamics can completely flip the sensitivity, so that it is the frequency fluctuations that are minimized.

The curve of measured and modeled operating points in Fig. 4 where the P1 frequency is minimized is initiated along a saddle-node bifurcation of limit cycles. In fact, at the end of the bifurcation the transition is between two limit cycles of different frequency. The laser switches from a limit cycle where the injected-shifted laser oscillation frequency is pushed away from the injection frequency at larger detuning to a limit cycle where the oscillation frequency is pulled towards the injection frequency for smaller detuning. This change in relative behavior of the system resonance relative to the injection frequency is necessary, though at higher injection levels we observe a smooth rather than abrupt transition. Further, we observe that the minimum P1 frequency merges with the bifurcation line as the difference between the two frequencies goes to zero. Frequency pushing behavior arises from the fact that the semiconductor laser is a detuned oscillator, while the frequency pulling behavior is the kind expected from an Adler-type analysis of an injected oscillator [8, 9]. At low injection levels, the saddle-node of limit cycle bifurcation starts at a P1 frequency and master laser frequency offset approximately equal to the characteristic relaxation resonance frequency of the free-running laser, separating the frequency-pushing and pulling regimes. At higher injection levels, where the sensitivity to perturbations is reduced, the local minimum of the P1 frequency is also a signature of a localized region of relative frequency pulling, or reduced absolute frequency pushing, of the injection-perturbed laser oscillation frequency.

At the high-injection level end of the operating points where the P1 frequency is minimized, the Hopf bifurcation is crossed at approximately the position where it deviates most strongly from the line $\omega = \xi$ that the bifurcation asymptotically approaches with increasing injection [10]. Therefore, we observe that the region of reduced sensitivity operation is bounded within a range where the attractor characteristics are different (frequency-pulling) from the P1 characteristics at larger detuning and away from the regions of complex dynamics and the saddle-node bifurcation of limit cycles (frequency pushing). Analysis of the P1 dynamics in terms of a solution with two dominant optical frequency components [11] cannot yield the localized minima of the P1 frequency with changes in the detuning. Similarly, a linearized analysis of the laser under stable injection locking [10] cannot yield such minima in this region, though they appear under the full nonlinear analysis [12]. Therefore, the P1 region and even the stable locking region can have attractors that yield dynamical features unexpected from perturbation solutions. Nonetheless, the full nonlinear model, Eqs. 1–3, recovers these features qualitatively/semi-quantitatively, with a proper accounting of the gain/refractive index saturation being necessary to quantitatively recover them in the optically-injected semiconductor laser.

In summary, we have presented experimental measurements and numerical calculations based on the coupled optical-field/carrier-density model of the optically-injected semiconductor laser that show the existence of specific operating points with reduced sensitivity to systematic fluctuations. These techniques complement and expand upon the recent use of specifically engineered nonlinear oscillators that used nonlinear dynamics to suppress oscillator phase noise [13, 14]. Further, the excellent agreement between model and experiment in this system makes it an ideal test configuration for investigating novel responses of a nonlinear system to external stimulus. More generally, the work highlights the nontrivial changes in the response of a nonlinear system to perturbations, and the fact that at specific operating points nonlinearly shifted perturbations are suppressed, while otherwise appearing to remain similar in characteristics to nearby operating points. This has technological relevance to the frequency reference application cited earlier, but we believe that such localized operating points may also be of importance to a wide range of nonlinear

systems.

The authors thank Prof. Thomas Erneux for a careful reading of an earlier version of this manuscript and for useful suggestions.

The work of T.B.S. and J.-M.L. was supported, in part, by the Air Force Research Laboratory through a contract with Optimetrics, Inc. The work of N.G.U. and V.K. was supported by Dr. Arje Nachman through an Air Force Office of Scientific Research grant (12RY09COR). The views and opinions expressed in this article are those of the authors and do not reflect the official policy or position of the United States Air Force, Department of Defense, or the U.S. Government.

* Corresponding author: Thomas.Simpson@L-3com.com

[1] S. H. Strogatz, *Nonlinear Dynamics and Chaos* (Westview Press, Cambridge, MA, 1994), 1st ed., ISBN 0738204536.

[2] T. Erneux and P. Glorieux, *Laser Dynamics* (Cambridge University Press, London, 2010), 1st ed., ISBN 0521830400.

[3] T. B. Simpson, Optics Communications **215**, 135 (2003), ISSN 0030-4018, URL http://www.sciencedirect.com/science/article/pii/S0030401802021922.

[4] S. Wieczorek, B. Krauskopf, T. Simpson, and D. Lenstra, Physics Reports **416**, 1 (2005), ISSN 0370-1573, URL http://www.sciencedirect.com/science/article/pii/S0370157305002656.

[5] See supplemental material at [URL will be inserted by publisher] for the formulation of Equations 1–3 from the coupled equation model, and the values of model parameters used in the calculations and their relation to physical parameters (2013), URL http://to~be~inserted~by~PRL.

[6] S.-C. Chan, S.-K. Hwang, and J.-M. Liu, Opt. Express **15**, 14921 (2007), URL http://www.opticsinfobase.org/oe/abstract.cfm?URI=oe-15-22-14921.

[7] Y. Yamamoto, S. Machida, and O. Nilsson, Phys. Rev. A **34**, 4025 (1986), URL http://link.aps.org/doi/10.1103/PhysRevA.34.4025.

[8] R. Adler, Proceedings of the IEEE **61**, 1380 (1973), ISSN 0018-9219.

[9] A. E. Siegman, *Lasers* (University Science Books, Salsuato, CA, 1986), 1st ed., ISBN 0935702113.

[10] T. Simpson, J. Liu, and A. Gavrielides, Quantum Electronics, IEEE Journal of **32**, 1456 (1996), ISSN 0018-9197.

[11] S.-C. Chan, Quantum Electronics, IEEE Journal of **46**, 421 (2010), ISSN 0018-9197.

[12] S.-K. Hwang, S.-C. Chan, S.-C. Hsieh, and C.-Y. Li, Optics Communications **284**, 3581 (2011), ISSN 0030-4018, URL http://www.sciencedirect.com/science/article/pii/S0030401811003373.

[13] E. Kenig, M. C. Cross, R. Lifshitz, R. B. Karabalin, L. G. Villanueva, M. H. Matheny, and M. L. Roukes, Phys. Rev. Lett. **108**, 264102 (2012), URL http://link.aps.org/doi/10.1103/PhysRevLett.108.264102.

[14] B. Yurke, D. S. Greywall, A. N. Pargellis, and P. A. Busch, Phys. Rev. A **51**, 4211 (1995), URL http://link.aps.org/doi/10.1103/PhysRevA.51.4211.